Structure-Reactivity Relationships of Buchwald-Type Phosphines in Nickel-Catalyzed Cross-Couplings

Samuel H. Newman-Stonebraker[1,2], Jason Y. Wang[1,2], Philip D. Jeffrey[3], Abigail G. Doyle*[1,2]

[1]Department of Chemistry, Princeton University, Princeton, New Jersey 08544, USA
[2]Department of Chemistry and Biochemistry, University of California Los Angeles, Los Angeles, California 90095, USA
[3]Department of Molecular Biology, Princeton University, Princeton, New Jersey 08544, USA

ABSTRACT: The dialkyl-*ortho*-biaryl class of phosphines, commonly known as Buchwald-type ligands, are among the most important phosphines in Pd-catalyzed cross-coupling catalysis. These ligands have also recently been applied to select Ni-catalyzed cross-coupling methodologies. However, little is known about their structure-reactivity relationships (SRRs) with Ni, and limited examples of well-defined, catalytically relevant Ni complexes with Buchwald-type ligands exist. In this work, we report the analysis of Buchwald-type phosphine SRRs in four representative Ni-catalyzed cross-coupling reactions. Our study was guided by data-driven classification analysis, which together with organometallic studies of structurally characterized Ni(0) and Ni(II) complexes and density functional theory allowed us to rationalize reactivity patterns in catalysis. Overall, we expect that this study will serve as a platform for further exploration of this ligand class in organonickel chemistry, as well as in the development of new Ni-catalyzed cross-coupling methodologies.

Introduction

Transition metal-catalyzed cross-couplings are among the most practical and widely used bond-forming reactions in the construction of small molecules.[1,2] The modern-day success of these methodologies is due in large part to ancillary ligand and precatalyst development, aided by thorough mechanistic investigations.[1,3] For Pd-catalyzed cross-couplings, the dialkyl-*ortho*-biaryl phosphines developed by Buchwald, Beller, and others has emerged as the ligand class of choice for many C–C and C–N bond-forming transformations.[4–8] Extensive mechanistic studies have been carried out to elucidate the structure-reactivity relationships (SRRs) of these phosphines with Pd (**Figure 1A**).[6,9–13] In brief, Buchwald-type ligands can promote the formation of highly reactive monoligated (L_1) Pd through increased steric pressure from the "B-ring" positioned within the metal's first coordination sphere. Additionally, they also can stabilize the unsaturated metal center via interactions with the phosphine's π-system (a pseudobidentate binding mode).[11,12,14,15] Most members of this ligand class are also characterized by a high degree of conformational flexibility, resulting in a wide range of attainable steric environments around the metal center (**Figure 1B**),[12,13] which can be limited by introducing groups on the A ring or increasing the size of the alkyl groups bound to phosphorus.[13,16] Overall, the design elements of these ligands promote challenging elementary steps while minimizing off-cycle speciation,[9,10] and allow for deactivated electrophiles such as aryl chlorides to be employed in catalysis with high levels of efficiency.

Over the past decade, Buchwald-type phosphines have also found successful application in a limited number of Ni-catalyzed cross-coupling reactions (**Figure 1C**).[17–25] One of the first reports came from our lab in 2011 with the development of a Ni-catalyzed cross-coupling of styrenyl epoxides and boronic acids, where BrettPhos was identified to be the most effective ligand in the transformation.[18] The Watson and Crudden labs have also reported the use of Buchwald-type phosphines in Ni-catalyzed-cross coupling reactions of naphthylic pseudohalides.[19,20] More recently, researchers at Bristol Myers Squibb identified CyJohnPhos as the most effective ligand for the Ni-catalyzed borylation of aryl halides, with other examples of the ligand class amongst the top performers.[21] Additionally, in a recent collaborative project carried out by our lab, the Sigman lab, and Merck & Co., Inc., we identified certain Buchwald-type phosphines as top performing among 90 diverse monophosphines for several Suzuki–Miyaura Coupling reactions (SMC) of aryl chlorides.[25]

While these examples illustrate that Buchwald ligands are capable of imparting desirable reactivity in Ni-catalyzed methodologies, little is known about their SRRs in Ni catalysis, or how their unique structure and binding modes interface with Ni more generally. A handful of computational studies have included Buchwald phosphines in their analyses, but the focus was not on the ligand class specifically.[26,27] Nicasio and coworkers have structurally characterized dialkylterphenyl phosphines on Ni; these ligands share certain attributes with Buchwald-type ligands.[28–30] However, to the best of our knowledge, only one example exists in the literature of a structurally-characterized Ni complex bound by a Buchwald phosphine: an off-cycle, cyclometalated adduct of BrettPhos formed during the cross-coupling of styrenyl epoxides.[18] Given the scarcity of relevant studies, insights into the SRRs and mechanism of Buchwald and CataCXium P phosphines in Ni catalysis, along with access to well-defined Ni complexes bearing these ligands, would be of great value both in the discovery of new methodologies and in the further understanding/optimization of existing ones.

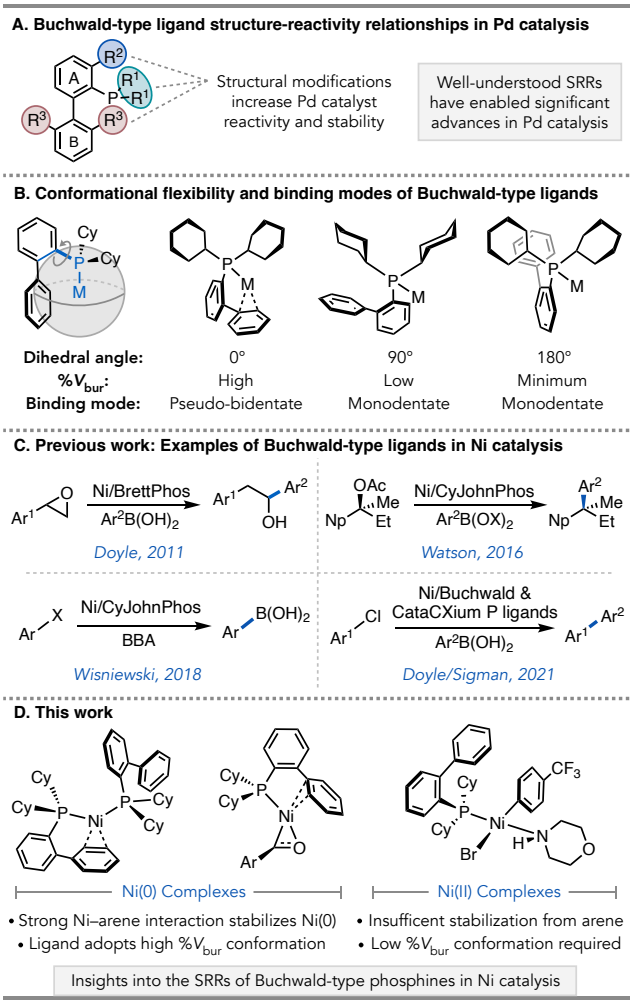

Figure 1. Introduction.

Herein, we report findings into the mechanism and SRRs of Buchwald-type phosphines in Ni cross-coupling catalysis, guided by data science, fundamental organometallic studies, and density functional theory (DFT) analysis. Four Ni-catalyzed cross-coupling datasets where Buchwald-type phosphines are active to varying degrees were used as case studies to explore catalyst structure and mechanism. Each of these cases provided insights into different elementary organometallic processes. The identification of percent buried volume (%V_{bur}) reactivity cliffs in several of these datasets allowed for interrogation of the specific ligand structural components that led to active (and inactive) catalysts.[25,31–33] Structural characterization and reactivity studies of new well-defined Ni(0) and Ni(II) complexes bound by Buchwald and CataCXium P phosphines were carried out for each of the reactions, allowing us to rationalize the observed reactivity patterns (**Figure 1D**). Overall, we expect the findings of this study will serve as a platform for the further exploration of organonickel chemistry with Buchwald-type ligands, enabling the rational use of this ligand class in new Ni-catalyzed methodologies.

Results and Discussion

%V_{bur} reactivity thresholds and catalytic case studies. At the outset of this study, we sought to use molecular features to describe the structure of Buchwald-type ligands in relation to their reactivity in Ni-catalyzed cross-couplings. To this end, Gensch et al. recently developed a comprehensive organophosphorus descriptor database, *kraken*, which contains conformationally informative electronic, steric, and whole-molecule DFT descriptors for 1558 unique monophosphines, including Buchwald-type ligands.[34] The descriptors generated for each ligand include the minimum, maximum, and Boltzmann-weighted average value for each feature across the phosphine's energetically accessible conformational ensemble, allowing for accurate representations of ligand structure relevant in coordination chemistry and organometallic catalysis. In our 2021 collaborative study with the Sigman lab and Merck & Co., Inc., we found that one of these conformationally representative descriptors, minimum percent buried volume (%V_{bur} (*min*)), afforded reactivity cliffs in Ni- and Pd-catalyzed cross-coupling datasets. Mechanistic studies revealed that a given phosphine's %V_{bur} (*min*) was linked to the spectroscopic formation of L_1M vs. L_2M catalysts, wherein the former was generally required for successful Pd catalysis, and the latter for successful Ni catalysis.[3,25,35]

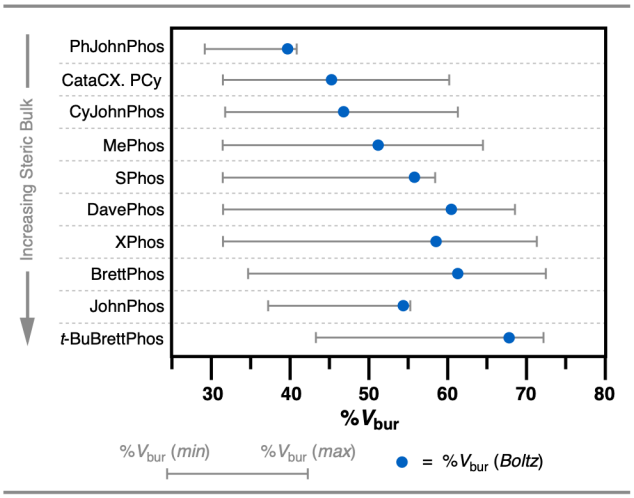

Figure 2. %V_{bur} range for select Buchwald and CataCXium P phosphines as defined by %V_{bur} (min) and %V_{bur} (max) from the *kraken* database. The Boltzmann-weighted %V_{bur} value is shown on the range as a blue dot.

While this workflow could be used to predict and rationalize the ligation state of Buchwald-type phosphines, it was not effective at capturing the catalytic reactivity behavior of these ligands. The large range of %V_{bur} values (**Figure 2**) and different binding modes (**Figure 1B**) attainable by these ligands explained their complex behavior in the Pd-catalyzed case studies,[36] but an understanding of their activity was less obvious for Ni.

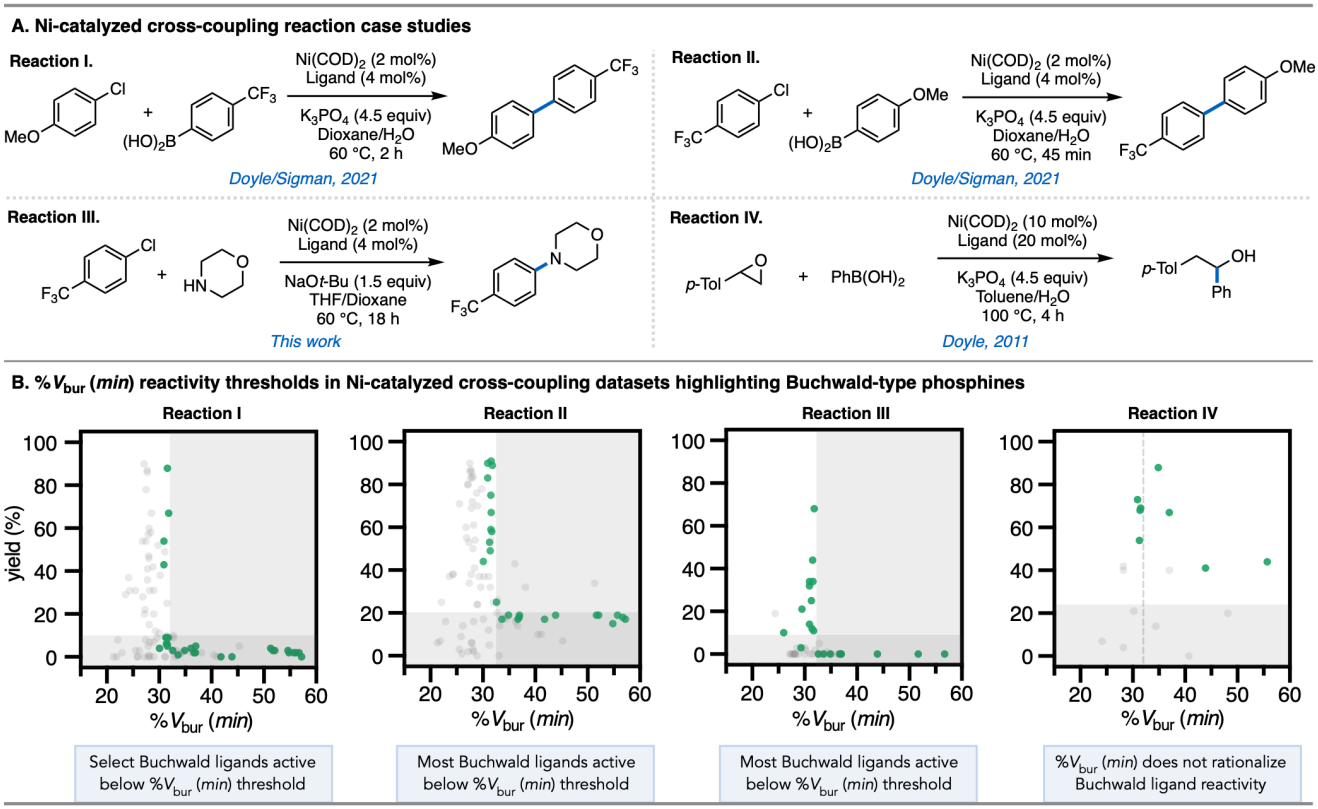

Figure 3. (A) Catalytic reactions studied. See SI for complete reaction conditions and procedures. (B) Buchwald-type ligand reactivity threshold analysis. Green dots represent Buchwald-type ligands. Grey dots are all ligands other than Buchwald-type screened in the reaction. The location of the horizontal gray box represents either ligandless background reactivity of $Ni(COD)_2$ or 10% yield, whichever is higher. The location of the vertical grey box represents the $\%V_{bur}$ (*min*) threshold decision. No threshold was located for Reaction IV.

For many Ni-catalyzed cross-coupling reactions promoted by monophosphines, including three of the five case studies examined in our previous $\%V_{bur}$ (*min*) threshold report, Buchwald-type ligands were entirely inactive. However, in other reactions, some Buchwald-type phosphines were among the best performers and the specific ones varied from reaction to reaction. These observations, combined with the fact that the Buchwald-type ligands were the only reactive ligands that favored L_1Ni(substrate) species raised questions about how they interact with Ni from both a structural and catalytic perspective.

Guided by reactivity threshold analysis, we assembled four Ni-catalyzed cross-coupling datasets as case studies (**Figure 3A**, Reactions **I-IV**), combining previously published (Reactions **I**, **II**, **IV**) and newly collected (Reaction **III**) datasets, wherein at least some Buchwald-type ligands were found to promote reactivity. These case studies, consisting of Csp^2–Csp^2 Suzuki–Miyaura couplings (Reactions **I** and **II**), a Csp^2–N coupling (Reaction **III**) of aryl chlorides, and a Csp^3–Csp^2 SMC of *p*-tol styrene oxide (Reaction **IV**), highlight stark differences in Buchwald ligand reactivity patterns, especially in the context of $\%V_{bur}$ (*min*) thresholds.

Case Study 1: Investigation of Ni(0) and oxidative addition in Suzuki–Miyaura Couplings. In the first case study, we examined Reaction **I**, an electronically mismatched SMC, wherein only four of the smallest Buchwald-type ligands screened (CyJohnPhos, CataCXium PCy, CataCXium PInCy, and CataCXium POMeCy) promoted reactivity. These four ligands fell on the left (reactive) side of a 32% V_{bur} (*min*) reactivity cliff (Figure 3B), but the descriptor alone did not distinguish the ligands from inactive Buchwald-type ligands with similar $\%V_{bur}$ (*min*) values, such as SPhos and XPhos. This is in contrast with Reaction **II**, where *all* Buchwald-type ligands screened with $\%V_{bur}$ (*min*) values less than 32% were reactive above ligandless control (**Figure 3B**). Since the reaction partners in Reaction II are activated, the difference in ligand response between **Reactions I** and **II** suggested to us that the four active ligands in Reaction **I** enabled the formation of a Ni species that could undergo a challenging elementary step of the catalytic cycle.

Scheme 1. Ni-catalyzed SMC Reaction Ib

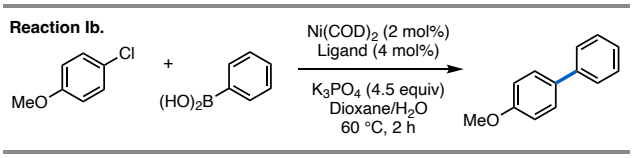

Examining Reaction **Ib**, a SMC employing the same 4-chloroanisole electrophile as Reaction **I** but an electron neutral phenyl boronic acid (**Scheme 1**), we found that the same four ligands as those identified in Reaction **I** were the only reactive Buchwald-type phosphines (see SI for threshold analysis), suggesting that the challenging step is oxidative addition into the electron-rich electrophile.[37,38] Therefore, we postulated that this step must require the preformation of a phosphine-ligated Ni(0) species *in situ* and only the four reactive phosphines are capable of reacting with the $Ni(COD)_2$ (COD = 1,5-cyclooctadiene) precursor to result in its formation.

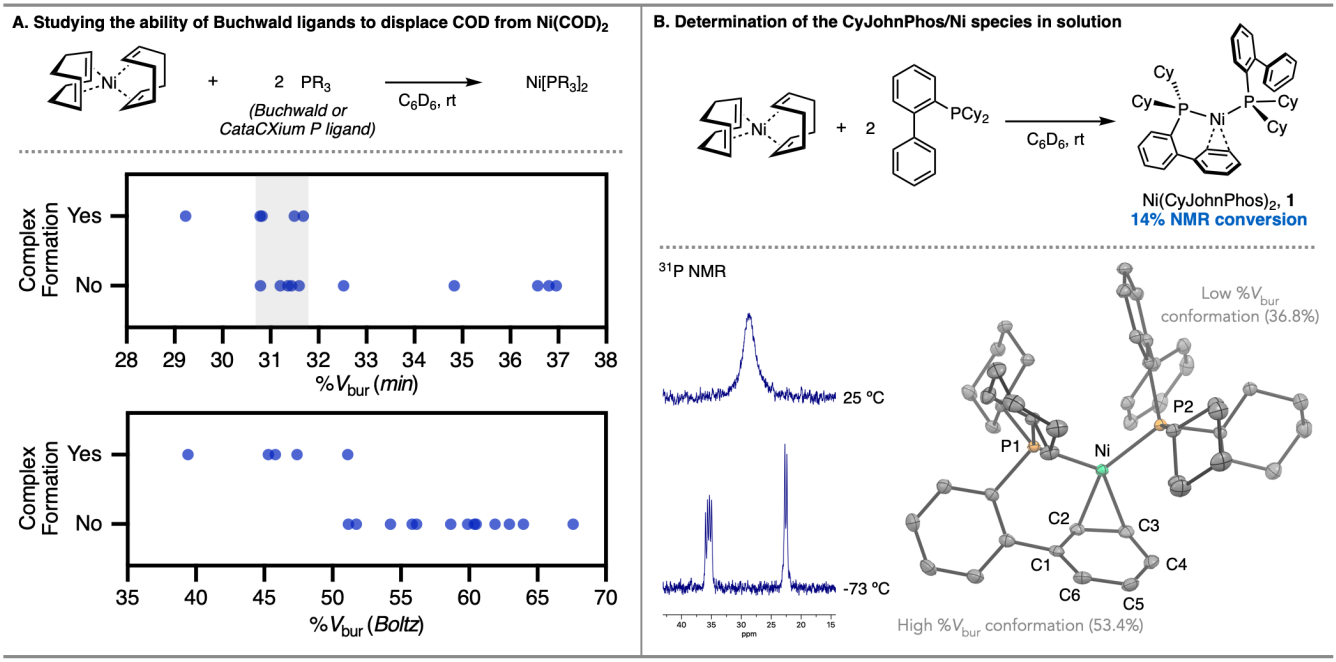

Figure 4. (A) Spectroscopic ligation experiment of Buchwald-type phosphines with $Ni(COD)_2$ (**Reaction V**). Complex formation determined by ^1H and ^{31}P NMR. (B) Structural characterization of $Ni(CyJohnPhos)_2$. Solid state structure with thermal ellipsoids at 50% probability shown. Hydrogen atoms omitted for clarity. Selected bond distances (Å): Ni–P1: 2.1905(5); Ni–P2: 2.1887(6); Ni–C2: 1.972(1); Ni–C3: 2.075(1); C1–C2: 1.444(2); C1–C6: 1.368(2); C2–C3: 1.426(2); C3–C4: 1.436(2); C4–C5: 1.361(2); C5–C6: 1.430(2).

To test this hypothesis, we subjected 18 Buchwald and CataCXium P ligands to stoichiometric reactions with $Ni(COD)_2$. ^{31}P and ^1H NMR spectra were analyzed to determine if the phosphine could form a new ligated complex *in situ* (**Figure 4A**). In these studies, we found that only the four active Buchwald-type ligands of Reaction **I** and **Ib** displaced COD spectroscopically to any appreciable degree.[39,40] None of the inactive Buchwald-type phosphines in Reaction **I**—those containing either *t*-Bu groups (e.g., JohnPhos) or significant steric bulk at the B ring *ortho* positions (e.g., SPhos, XPhos)—were found to bind. We then investigated the ability of ligand steric descriptors to rationalize COD displacement/complex formation. In alignment with the catalytic results for Reaction **I**, $\%V_{bur}$ (*min*) alone could not distinguish ligands that formed complexes from those that did not. However, $\%V_{bur}$ (*Boltz*)—an energy-weighted representation of the ligand's average overall size—was quite successful: only ligands with $\%V_{bur}$ (*Boltz*) values less than 52% formed complexes under the conditions (**Figure 4A**).

We sought to structurally characterize a representative example of these species using single crystal X-ray diffraction (SCXRD) analysis. Despite the low conversion, we obtained single crystals of the CyJohnPhos Ni complex (co-crystallized with unreacted $Ni(COD)_2$) by cooling a reaction solution in pentane to –78 °C. The crystal structure of **1** revealed two CyJohnPhos ligands bound to Ni: one with a relatively low $\%V_{bur}$ conformation (36.8 %) with κ^1-P (monodentate) binding, and the other as a high $\%V_{bur}$ conformation (53.4%) with κ^1-P,η^2-C_{arene} (pseudobidentate) binding and evidence of substantial backbonding into the arene (**Figure 4B**), resulting in a formally 16 e^- Ni(0) species.[29,41,42] The Ni-arene interaction in **1** is significantly more pronounced than that of the analagous $Pd(CyJohnPhos)_2$ complex reported by Fink and coworkers.[15]

To study the reactivity of **1** further, along with the analogous complexes of the three other reactive ligands from **Reaction I**, we tested synthetic strategies to afford the complexes in the absence of COD or other pi-accepting ligands that commonly support Ni(0) precursors.[3,43–45] We were pleased to find that the reduction of $Ni(acac)_2$ with $AlMe_3$ in the presence of 2 equivalents of ligand gave **1** in good yield. The strategy was successfully applied to synthesize Ni(CataCXium $PCy)_2$ (**2**), Ni(CataCXium $PInCy)_2$ (**3**), and Ni(CataCXium $POMeCy)_2$ (**4**) (**Scheme 2**). **2-4** were also characterized using SCXRD, and their structure and bonding were similar to **1** (see SI for structural details).

Scheme 2. Synthesis and isolation of $L_2Ni(0)$ complexes[a].

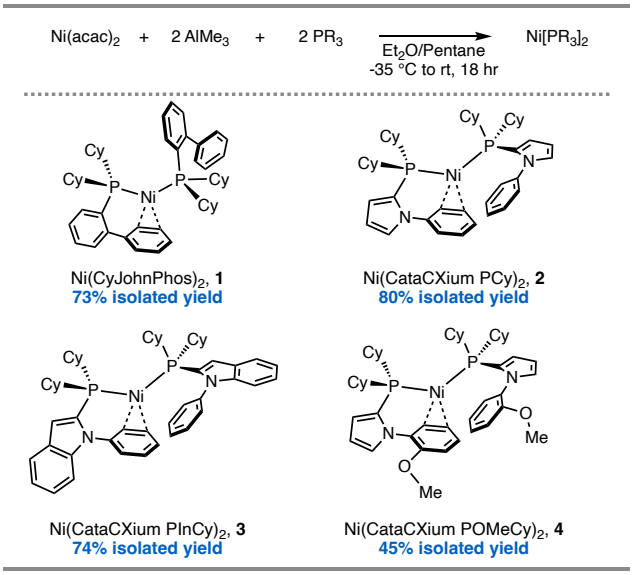

[a]X-ray structures of **2-4** can be found in the SI.

Based on these structures, the $\%V_{bur}$ (Boltz) threshold for complex formation can be rationalized, as the pseudobidentate ligand must not be so large that it crowds out Ni's first coordination sphere to prevent the monodentate ligand from favorably binding. Indeed, **3** was the only example of this complex class we were able to access with any *ortho*-substitution on the B ring. Furthermore, the reduction strategy did not allow us to access analogous structures with bulkier phosphines, with only decomposition or formation of unidentified/non-isolable species observed by NMR. Thus, the $\%V_{bur}$ (*Boltz*) Ni[PR_3]$_2$ complex-formation threshold observed in **Figure 4A** seems to extend beyond reaction with Ni(COD)$_2$, and may reflect complex stability more generally.

Testing **1**-**4** in catalysis, we were excited to find that all four were active precatalysts in Reaction **I**, consistent with the requirement for attaining the pre-ligated Ni(0) species to initiate the catalytic cycle (see SI for details). Isolation of these species also gave us the ability to study oxidative addition stoichiometrically. We hoped that a better understanding of this step, in addition to identification of Buchwald-type ligand-bound Ni(II) species that formed after oxidative addition, would allow us to mechanistically rationalize the $\%V_{bur}$ (*min*) reactivity cliffs observed across **Reactions I-III**.

Studying oxidative addition with CyJohnPhos$_2$Ni(0). Using **1** as a model complex, we performed a stoichiometric oxidative addition reaction with 2 equivalents of 2-chloro-5-fluorotoluene at room temperature and monitored the reaction by ^{31}P and ^{19}F NMR. A ^{31}P resonance consistent with a new diamagnetic CyJohnPhos-bound Ni species was observed within minutes, and conversion of the aryl chloride was concurrently observed by ^{19}F NMR. Interestingly, the new ^{19}F resonance that predominantly formed (with good mass balance) matched that of 3-fluorotoluene. Minimal conversion to other species that would be consistent with aryl-bound Ni was observed. Furthermore, after one hour and complete conversion of **1**, > 50% (relative to Ni) of the aryl chloride remained, and a substantial amount of Ni black and free phosphine were observed (**Figure 5A**).[46]

The effects of ligand stoichiometry on oxidative addition were then examined by conducting the reaction in the presence of 10 equivalents of free CyJohnPhos. The addition of free ligand did not substantially affect the overall conversion of **1** and aryl chloride, and the same products were observed spectroscopically. This suggests that excess free ligand does not stabilize or trap reactive species to prevent decomposition to a great extent. However, the additional free ligand substantially increased the time needed to reach full conversion of **1** (and maximum conversion of the aryl chloride) compared with the reaction where no free ligand was added, implicating the intermediacy of L$_1$Ni(0) species prior to and/or during the oxidative addition step (see SI).

Density functional theory (DFT) studies were used to supplement our experimental results of the oxidative addition of **1** into aryl chlorides. Consistent with the finding that excess free ligand inhibits oxidative addition, we found that the dissociation of one equivalent of CyJohnPhos from **1** resulted in an 18 e$^-$ L$_1$Ni(0) species with an η^6-arene interaction between the Ni and the CyJohnPhos B-ring (intermediate **i**, **Scheme 3**).[47,48] A ΔG_{dissoc} of 13.9 kcal/mol was found at the M06/def2-TZVP//B3LYP-D3/6-31G(d,p) (SDD for Ni) level of theory. Following complexation of the aryl chloride to the L$_1$Ni species,[27] a C–Cl bond cleavage transition state was found with an energy of 25.9 kcal/mol relative to **1** (12.0 kcal/mol relative to **i**), with interactions between the Ni and B-ring stabilizing the otherwise unsaturated species. Interestingly, despite the high degree of unsaturation of the resulting 14 e$^-$ oxidative adduct **ii** (**Scheme 3**), no strong stabilizing interaction between the Ni and arene was observed computationally. Dimerization of **ii** and formation of the L$_2$Ni(II) oxidative adduct were both computed to proceed to species slightly downhill of **ii**. However, given that none of these species were consistent with the spectroscopic analysis of the resulting oxidative addition product, we postulated that **ii** must form a new complex via a decomposition pathway in the absense of other substrates or ligands.

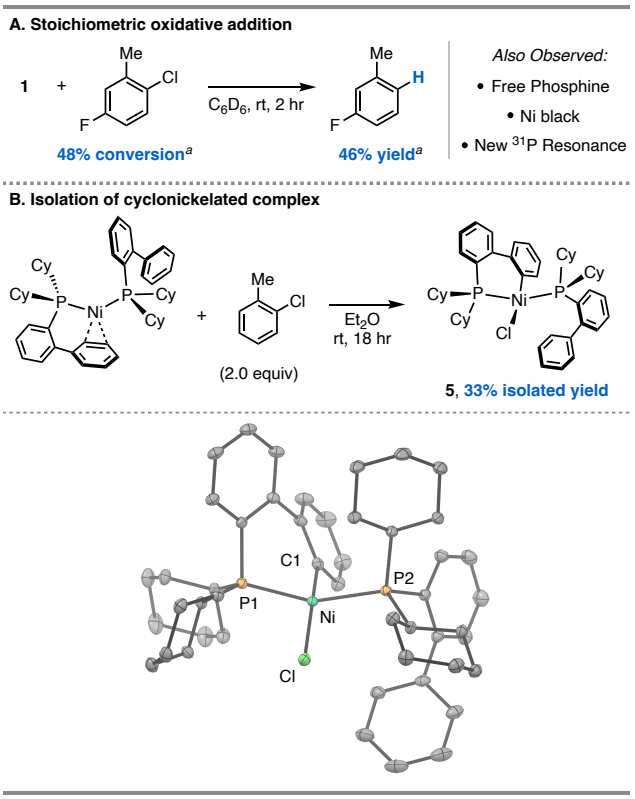

Figure 5. (A) Spectroscopic evaluation of the oxidative addition of **1** to 2-chloro-5-fuorotoluene. 2.0 equiv of 2-chloro-5-fluorotoluene used relative to **1**. [a] Conversion and yield are relative to 1.0 equiv of **1** and were determined using ^{19}F NMR using a 2-Fluorobiphenyl internal standard. (B) Isolation of cyclometalated CyJohnPhos Ni(II) adduct. Thermal ellipsoids displayed at 50% probability. Hydrogen atoms omitted for clarity. Selected bond distances (Å): Ni–P1: 2.1863(4); Ni–P2: 2.2628(4); Ni–C1: 1.908(1); Ni–Cl: 2.2192(3).

To identify the new Ni species observed *in situ* by ^{31}P NMR, oxidative addition of **1** with 2-chlorotoluene was then carried out on larger scale. We isolated and crystallized the resulting air-stable species (**5**) and analyzed it by SCXRD (**Figure 5**). The crystal structure of **5** confirmed that the aryl from the electrophile was not bound to Ni, and that one equivalent of CyJohnPhos had undergone a C–H activation and concurrent cyclonickelation. While this type of catalyst deactivation is well known with Pd for ligands without 2,6-substituted B-rings, for the C–H activation to occur with Ni rapidly, under such mild conditions, and with a non-chelating ligand is remarkable.[49–57] It is also notable that this

cyclometalation occurs significantly faster than in the analagous CyJohnPhos/Pd system reported by Fink.[15] Computationally, we were unable to locate a reasonable transition state from **ii**, the L_2Ni(II) structure, or the μ-Cl dimer that would lead to **5**.[58] Additional experimental and computational investigations into the mechanism and implications of this pathway are underway.

Scheme 3. Proposed catalytic cycle for Ni-catalyzed SMCs with CyJohnPhos.[a]

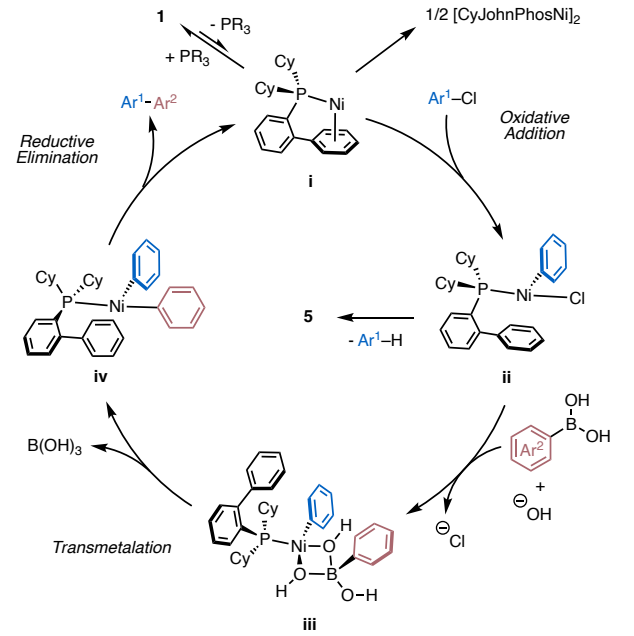

[a]See SI for reaction free energy profile.

In summary, only the smallest Buchwald-type ligands—those that possess minimal B-ring substitution and alkyl groups smaller than *t*-Bu—are capable of displacing COD from Ni(COD)$_2$ and forming Ni[PR$_3$]$_2$ species. The ability to form these complexes *in situ* in Reaciton **I** was required to activate the electron-rich aryl chloride and undergo oxidative addition. However, in the absense of other reaction components, the resulting coordinatively unsaturated Ni(II) complex is susceptable to decomposition and off-cycle pathways, particularly with the lack of protective B-ring 2,6-substitution.[9,10]

Case Study 2: Investigation of SRRs at Ni(II) in Ni-catalyzed SMCs. While the stoichiometric oxidative addition with the aryl chloride partner alone proceeded inefficiently and ultimately led to deactivation/decomposition of the Ni catalyst, the catalytic SMC reactions proceeded with turnover numbers (TONs) greater than 30. This suggests that other components of the reaction can trap intermediate **ii**, prevent decomposition pathways, and ultimately drive the reaction to turnover. Unfortunately, we were unable to study the transmetalation step experimentally due to difficulties synthesizing the relevant CyJohnPhos-bound Ni(II) oxidative adducts containing halides (*vide supra*) or hydroxide, coupled with the highly reactive nature of boronic acid/boronate–Ni complexes. However, we were able to computationally study the elementary step, along with the remainder of the catalytic cycle (**Scheme 3**).[59]

By DFT, the reaction of intermediate **ii** and trihydroxy(phenyl)borate to displace chloride was found to proceed favorably (-2.4 kcal/mol from II) to intermediate **iii**, a four-coordinate, 16 e$^-$ 8-B-4 species (**Scheme 3**).[59–61] The transition state of B-to-Ni transmetalation was found at 12.3 kcal/mol above **ii**, resulting in L_1Ni(aryl)$_2$ intermediate **iv**, which was computed to readily undergo reductive elimination to regenerate **i** and drive the reaction forward. Additionally, a four-coordinate, 16 e$^-$ L_1 μ-OH dimer complex with CyJohnPhos was investigated computationally.[59,62] While it is likely an off-cycle species that must be broken up prior to transmetalation, its stability (43.3 kcal/mol lower than **ii** + $^-$OH) may serve to trap **ii** and prevent cyclonickelation during catalysis.[63]

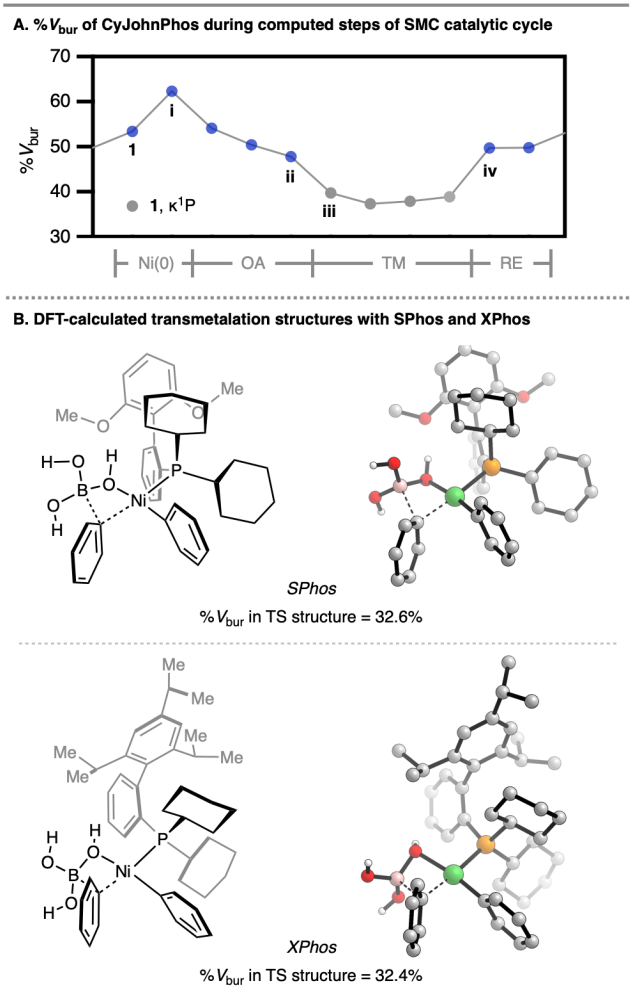

Figure 6. (A) %V_{bur} of CyJohnPhos during the DFT-optimized steps of the SMC catalytic cycle at the M06/def2-TZVP//B3LYP-D3/6-31G(d,p) [SDD] level of theory (see SI for details). Blue dots represent conformers where B ring is occupying second coordination site, gray dots represent a conformation of CyJohnPhos where the B-ring is > 3.0 Å away from Ni (monodentate). (B) DFT-optimized B-to-Ni transmetalation transition state structures with SPhos and XPhos. All %V_{bur} calculations performed using SambVca 2.1.

Re-examining the proposed SMC cycle in the context of the reactivity thresholds observed in **Reactions I** and **II**, we calculated the %V_{bur} values of CyJohnPhos in the DFT-generated intermediates and transition states. Unsurprisingly,

the %V_{bur} values of CyJohnPhos in the intermediates prior to and after transmetalation were near to or greater than 50%, consistent with the B-ring fully occupying a coordination site on Ni. However, during the steps of transmetalation, the boronic acid (or OH^- in the case of the μ-OH dimer) occupies two of four coordination sites in the square plane, forcing the B-ring to swing away from Ni, lowering the %V_{bur} of the ligand to 35-39% (**Figure 6A**).[64] Thus, the mechanistic rationale most consistent with the observed reactivity thresholds is the need for ligands to attain conformations wherein they will occupy only one of Ni's coordination sites, allowing for both the stabilization of Ni(II) by additional σ-donor ligands and key binding events of substrates.

Buchwald-type ligands with B-ring substitution and %V_{bur} (*min*) values less than 33% (e.g., SPhos and XPhos) were also reactive in **Reaction II**, despite their inability to react with $Ni(COD)_2$ on their own. Given the high amount of ligandless background reactivity in this reaction and the activated, electron-deficient nature of the aryl chloride, it is likely that the electrophile reacts directly with $Ni(COD)_2$. The phosphine would then bind later in the catalytic cycle (i.e., at Ni(II)) to facilitate transmetalation and reductive elimination. In studying SPhos and XPhos computationally at Ni(II), their ability to adopt conformations with the substituted B-ring rotated entirely behind the phosphorus lone pair/cyclohexyl rings (%V_{bur} values ~32%) enabled favorable boronic acid binding and transmetalation (**Figure 6B**) with the phosphine bound. While we were unable to obtain X-ray structures of these intermediates with Ni, this analysis and interpretation is consistent with structural evidence of SPhos and XPhos on Pd, wherein they often adopt low %V_{bur} conformations on Pd(II) with an additional σ-donor ligand bound.[65,66] However, for Buchwald-type ligands that possess either *t*-Bu groups bound to phosphorus (e.g., JohnPhos) and/or substitution on the A-ring (e.g., BrettPhos)—both modifications reflected by increased %V_{bur} (*min*) values—the inability to adopt truly monodentate structures appears to impede their successful use in Ni-catalyzed SMC reactions of aryl halides and boronic acids.

Case Study 3: Buchwald-type ligand reactivity in a Ni-catalyzed C–N coupling. Over the past decade, significant advancements have been made in methodology development of Ni-catalyzed C–N couplings, which are most commonly facilitated by bisphosphines.[67–73] While monophosphines generally do not promote reactivity in these reactions, a screen of monophosphines in **Reaction III**—a C–N coupling of 4-chlorobenzotrifluoride and morpholine (**Figure 3A**)—revealed that that several Buchwald-type ligands were uniquely capable of promoting catalytic reactivity. The reaction exhibited a similar %V_{bur} (*min*) reactivity threshold with Buchwald-type phosphines as **Reaction II**, though no ligandless background reactivity was observed, resulting in a much more pronounced reactivity cliff (**Figure 3B**). Other than Buchwald and CataCXium P ligands, only the smallest monophosphines screened (e.g., PEt_3) promoted the reaction to any appreciable degree (<20%).[74] This indicates that Buchwald-type ligands are priviledged amongst monophosphines in this reaction, with CyJohnPhos the top performer.

Given that the first steps of the catalytic cycle of **Reaction III** should be nearly identical to those of SMC **Reactions I** and **II**, we began by studying the effects of the amine on complexation following oxidative addition. Specifically, we were interested to observe if the presence of the σ-donor ligand could trap **ii** (**Scheme 3**) and form a stable 16 e^- complex, preventing cyclonickelation and other decomposition pathways. We were excited to find that the stoichiometric oxidative addition reaction of **1** with 4-chlorobenzotrifluoride, as well as with 2-chloro-5-fluorotoluene (*vide supra*), proceeded efficiently to a new Ni complex that was spectroscopically consistent with a Ni(II) oxidative adduct containing both the phosphine and the aryl group. Minimal evidence of cyclonickelation or other decomposition products were observed, indicating that the σ-donating morpholine was indeed capable of trapping **ii**, preventing decomposition (**Figure 7A**).

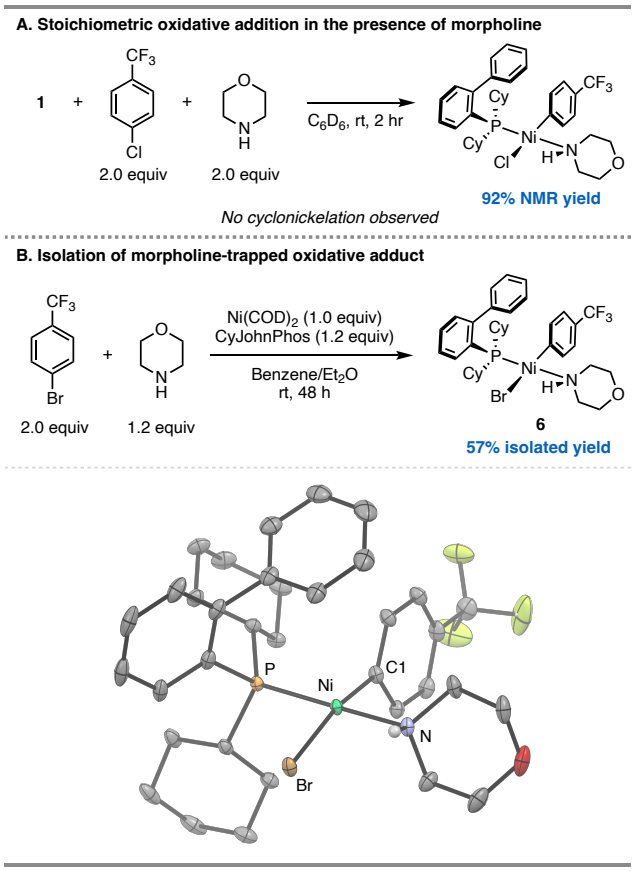

Figure 7. (A) Oxidative addition of 4-chlorobenzotrifluoride into **1** in the presence of morpholine. Yield determined by ^{19}F NMR with a 2-fluorobiphenyl internal standard. **(B)** Isolation of morpholine trapped oxidative adduct with CyJohnPhos. Solid state structure with thermal ellipsoids at 50% probability shown. All hydrogen atoms bound to carbons omitted for clarity. Selected bond distances (Å): Ni–P: 2.1906(5); Ni–N: 1.993(1); Ni–C1: 1.881(1); Ni–Br: 2.4119(5).

Due to the presence of excess free phosphine when starting from **1**, we opted to isolate a representative morpholine-bound Ni complex from $Ni(COD)_2$, two equivalents 4-boromobenzotrifluoride, and a slight excess of both CyJohnPhos and morpholine. This reaction successfully afforded **6** (**Figure 7B**) in 56% yield. We were able to characterize **6** by SCXRD, structurally confirming that morpholine had trapped the oxidative adduct as a stable four-coordinate 16 e^- complex,[65,75] preventing the cyclonickelation pathway. Similar to the DFT-optimized structures during SMC transmetalation, the B-ring of CyJohnPhos in **6** had rotated out of the first coordination sphere almost entirely and adopted a

relatively low %V_{bur} conformation of 37.3%. A favorable C–H π interaction between the Ni-bound aryl and the B-Ring of CyJohnPhos stabilized this slightly higher %V_{bur} conformation (see SI for details).

Scheme 4. Stoichiometric C–N Reductive Elimination and Precatalyst Studies with 6.

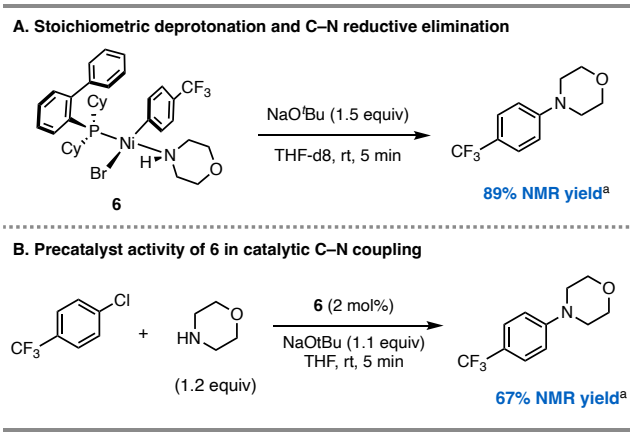

[a]NMR yield relative to 1-fluorobiphenyl internal standard. [b]GC yield relative to dodecane internal standard.

Access to **6** gave us a unique opportunity to stoichiometrically observe and study N–H deprotonation and subsequent C–N reductive elimination from a catalytically on-cycle amine-bound Ni complex.[76,77] We found that combining **6** with a slight excess of NaO*t*-Bu in a stoichiometric NMR study under inert atmosphere gave C–N coupled product in 89% NMR yield (**Scheme 4A**), which had reached maximum conversion by the time the spectrum was taken (< 5 minutes). This indicates that the deprotonation and reductive elimination steps occurred rapidly, even at room temperature, suggesting that C–N bond-forming transition state barrier from the deprotonated complex is low. We also tested **6** as precatalyst in **Reaction III**. We were pleased to find that it was a reactive precatalyst in the reaction, with about 30 turnovers observed within minutes, even at room temperature (**Scheme 4B**).

DFT studies showed that the reductive elimination barrier from the Ni amido species (intermediate **vi, Scheme 5**) is 13.3 kcal/mol, consistent with the experimental observation. The B-ring of the arene rotated back to block the fourth coordination site during reductive elimination, ultimately forcing the coupling partners *cis* on Ni's square plane. However, no strong interaction was observed computationally between the arene and the metal during this step.

Attempts to isolate complexes analogous to **6** with SPhos and XPhos were unsuccessful despite their reactivity in **Reaction III**. For both, *in situ* NMR studies of the stoichiometric oxidative addition in the presence of morpholine did indicate that a new phosphine-ligated Ni(II) complex formed, albeit in low yields (see SI).By DFT, these complexes likely had phosphines bound with %V_{bur} values close to 32%, allowing for the fourth coordination site to be accessed by the amine. While these phosphine-ligated complexes are attainable in spectroscopic studies and in catalysis, the only species that we could isolate and crystalize was **7** (**Scheme 6**).[78]

Scheme 5. Proposed catalytic cycle of Ni-catalyzed C–N coupling with CyJohnPhos.[a]

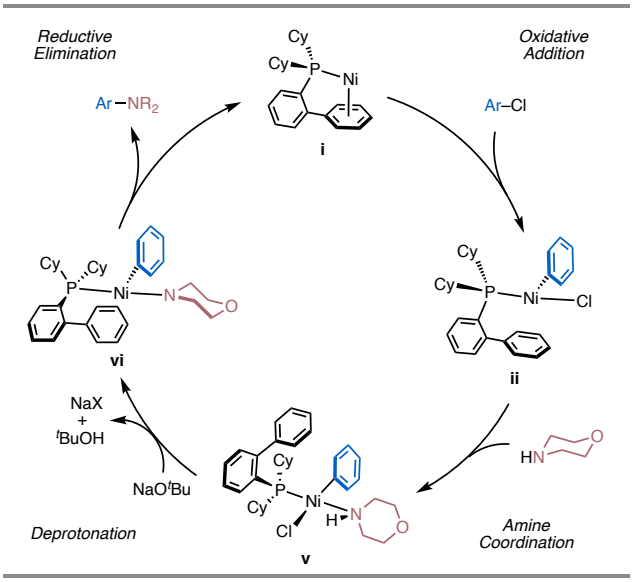

[a]See SI for reaction free energy profile.

Furthermore, this catalytically inactive bis-morpholine ligated complex was the exclusive oxidative addition product observed with Buchwald-type phosphines possessing %V_{bur} (*min*) values >32%. In addition to allowing access to the additional coordination site for amine binding, the %V_{bur} (*min*) reactivity threshold in **Reaction III** could also be reflective of congested transition states during substrate deprotonation and/or ligand substitutions with *tert*-butoxide, where Ni's first coordination sphere may be required to be unencumbered by the phosphine.

Scheme 6. Outcome of oxidative addition with phosphines having %V_{bur} (*min*) values >32%[a].

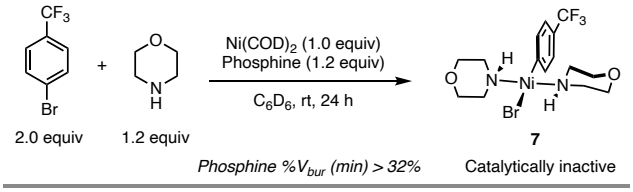

[a]X-ray structure of **7** can be found in the SI.

To summarize our findings from this case study, σ-donating amine substrates can bind to and stabilize L_1Ni oxidative adducts with Buchwald-type ligands. However, the B ring of the phosphine must rotate out of the first coordination sphere in order for the coordination site to be accessed by the amine, which requires no A-ring substitution and alkyl groups smaller than *t*-Bu. The resulting 16 e$^-$ complexes, such as **6**, rapidly undergo deprotonation and C–N bond-forming reductive elmination at room temperature in the presence of base, and show exciting promise as precatalysts for these reactions.

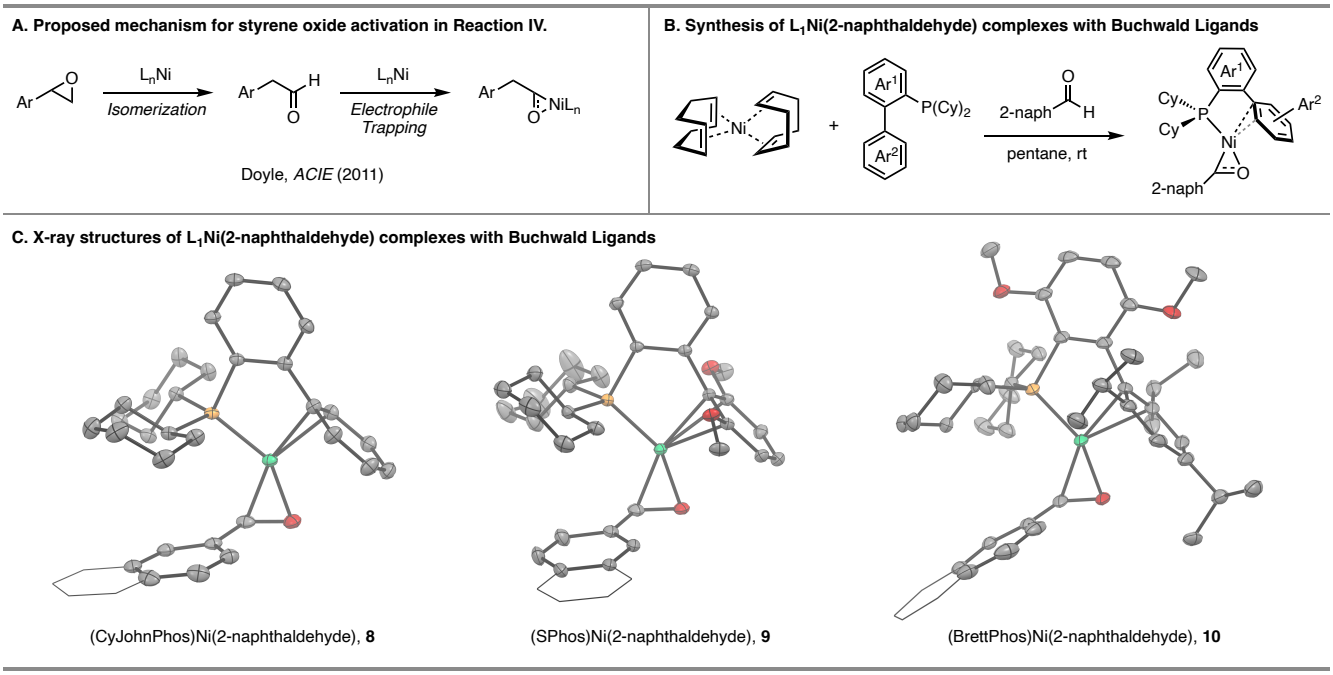

Figure 8. (A) Activation of styrene oxide in **Reaction IV** proposed by Nielsen and Doyle. (B) Synthesis of L_1Ni(2-naphthaldehyde) complexes with Buchwald ligands from $Ni(COD)_2$. (C) X-ray crystal structures of L_1Ni(2-naphthaldehyde complexes with CyJohnPhos, SPhos, and BrettPhos. Thermal ellipsoids displayed at 50% probability for **8** and **9**, and 30% probability for **10**. Hydrogen atoms omitted for clarity.

Case study 4: Structural studies of Ni(0) aldehyde complexes with Buchwald-type ligands. In the final case study, we investigated **Reaction IV**, which was reported by our laboratory in 2011. In the original study, it was found that the use of Buchwald-type ligands was necessary to enable high reactivity, and that bulky BrettPhos was the highest performing example tested.[18] Re-evaluating the ligands screened in the reaction, no $\%V_{bur}$ (*min*) reactivity threshold was observed, and Buchwald-type ligands of all steric profiles were active above background reactivity (**Figure 3B**). Unlike the previous case studies, this transformation is an example of a cross-coupling reaction of an unconventional electrophile, where the standard elementary steps of Csp^2–X activation/oxidative addition do not necessarily apply. Specifically, the mechanism of styrene oxide activation was proposed by Nielsen and Doyle to first proceed through isomerization, generating phenylacetaldehyde *in situ*, followed by Ni complexation and arylation; notably, the reaction was found to proceed directly from phenylacetaldehyde (**Figure 8A**), though from a methodological standpoint, styrene oxide was the preferred electrophile.[18]

In the original report, an off-cycle intermediate of the isomerization pathway was isolated, with Ni(II) bound to the 4-position of the dearomatized B-ring of BrettPhos. To the best of our knowledge, this represented the only other structurally characterized Ni complex with a Buchwald ligand before this study. However, subsequent trapping of the aldehyde was not investigated, and it remained unclear how the ligand interacted with Ni structurally during this step. Recently, we used 4-flurobenzaldehyde to spectroscopically determine the ligation state of Ni with various phosphines, including Buchwald-type phosphines. The stability of the complexes in solution suggested that benzaldehyde derivatives may provide a stable trap for both L_2Ni and L_1Ni species, allowing for the study and isolation of L_1Ni(aldehyde) complexes with Buchwald ligands.[25] Indeed, we found that most Buchwald-type ligands, regardless of their $\%V_{bur}$ values, could form L_1Ni(4-Fluorobenzaldehyde) complexes spectroscopically from $Ni(COD)_2$ (**Figure 9**). The two exceptions were (*t*-Bu)BrettPhos and (*t*-Bu)XPhos, whose considerable steric bulk prevented ligation altogether. However, certain Buchwald ligands with *t*-Bu groups bound to phosphorus that had no B-ring substitution (e.g., JohnPhos) or mono B-ring substitution (e.g., (*t*-Bu)MePhos) could complex spectroscopically.

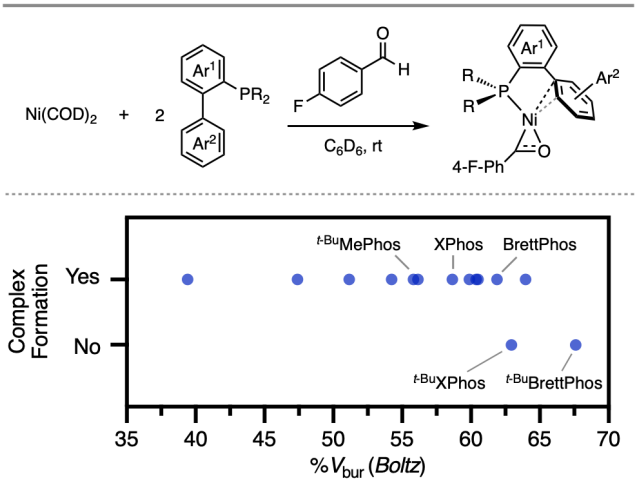

Figure 9. Spectroscopic complex formation studies with 4-F-benznaldehyde (**Reaction VI**). Complex formation determined by ^1H, ^{19}F, and ^{31}P NMR

Given that no $\%V_{bur}$ (*min*) steric threshold was observed in **Reaction IV** or in the spectroscopic experiments with 4-Fluorobenzaldehyde, we hypothesized that the ligands would adopt high $\%V_{bur}$ conformations (with the B ring fully occupying a coordination site) when bound to Ni-aldehyde

complexes. For ease of synthesis and crystallization, 2-naphthaldehyde was chosen to isolate complexes bearing a selection of phosphines: CyJohnPhos, SPhos, and BrettPhos (**8**-**10**, **Figure 8C**). For each of the three complexes, the X-ray structure revealed that the B-ring of the phosphine was indeed fully occupying a coordination site on Ni, with ligand $\%V_{bur}$ values of 53.2%, 56.0%, and 60.7% for **8**, **9**, and **10**, respectively. Thus, for these complexes, the phosphine occupies more than 50% of Ni's first coordination sphere/two of four coordination sites, preventing additional ligand or substrate equivalents from binding. While less π-basic than the Ni centers of **1**-**4**, stabilizing η^2-C_{arene} interactions (η^1-C_{arene} in the case of **9** with SPhos) are still present to result in 16 e^- Ni(0) species, with indications of backbonding into the B-ring evident through C–C bond elongations and distortions.

We were pleased to find that the BrettPhos complex **10** was an active precatalyst in **Reaction IV**, suggesting that it is an on-cycle species. While the exact mechanism of aldehyde arylation from the boronic acid coupling partner is still unclear, the observation that the most active ligands were those that enforce occupation of two coordination sites suggests the 1,2 arylation pathway may not proceed through a traditional B-to-Ni transmetallation (*vide supra*).[79] Further investigations are underway to explore the mechanism and methodological implications in greater detail.

Summary & Conclusion

Using $\%V_{bur}$ threshold analysis alongside mechanistic organometallic investigations, we have elucidated the structure-reactivity relationships of Buchwald-type ligands in four representative Ni-catalyzed cross-coupling reactions. A summary of our findings related to the bonding, speciation, and SRRs of Buchwald-type ligands at Ni(0) and Ni(II) is below.

Ni(0):

- Ni(0) complexes can form stabilizing η^2-arene interactions with the B-ring of Buchwald-type ligands.
- Ligands that posess minimal B-ring substitution and alkyl groups smaller than *t*-Bu—reflected by both relatively low $\%V_{bur}$ (*min*) and $\%V_{bur}$ (*Boltz*) values—can form Ni[PR_3]$_2$ complexes *in situ* from Ni(COD)$_2$. These complexes can undergo oxidative addition to aryl halide electrophiles.
- In these 16 e^- complexes, one of the two phosphines adopts a high $\%V_{bur}$/pseudobidentate conformation with η^2-C_{arene} binding, and the other adopts a low $\%V_{bur}$/monodentate conformation. Because of this arrangement, the ligands must be small enough to not overcrowd the complex.
- In the presence of π-accepting substrates like aldehydes that can react with Ni(COD)$_2$ on their own, most Buchwald-type ligands, including those that have B-ring substitution and/or *t*-Bu groups, readily bind to form L_1Ni(substrate) complexes. Stabilizing interactions are observed between the π-basic Ni center and B-ring, resulting in 16 e^- Ni(0).
- In this scenario, the ligand adopts a high $\%V_{bur}$/pseudobidentate conformation, and no $\%V_{bur}$ (*min*) steric threshold is observed. However, ligands that have both 2,6-substitution on their B-ring and *t*-Bu alkyl groups are too bulky to form stable complexes.

Ni(II):

- At less π-basic Ni(II), weaker interactions between the Ni and B-ring arene are insufficient to stabilize coordinatively unsaturated oxidative addition complexes. The σ-donating substrate must bind to the L_1Ni(II) oxidative adduct to both stabilize the otherwise 14 e^- complex and to facilitate catalytic turnover.
- The B-ring of the phosphine must rotate out of the first coordination sphere to enable substrate binding. Alkyl groups smaller than *t*-Bu and no A-ring substitution—reflected by relatively low $\%V_{bur}$ (*min*) values—are required to enable these fully monodentate conformations of Buchwald-type ligands.
- For ligands with low $\%V_{bur}$ (*min*) values but with 2,6 substitution (e.g., SPhos and XPhos), substrate binding and catalytic turnover occurred, but the higher energetic penalty of attaining these fully monodentate conformers decreased stability and catalytic efficiency.

In the context of the catalytic reactions studied, ligands with minimal substitution, such as CyJohnPhos and CataCXium PCy, were the most effective Buchwald-type phosphines at promoting cross-coupling of aryl halides. The ability of these ligands to readily adopt both high and low $\%V_{bur}$ conformations gives rise to hemilability (pseudobidentate at Ni(0) and monodentate at Ni(II)), which appears to be desirable in these Csp^2–Csp^2 and Csp^2–N bond-forming reactions. For reactions of unconventional cross-coupling electrophiles that involve π-complexes, larger, less conformationally flexible ligands like BrettPhos are viable candidates to promote a successful transformation.

Overall, we expect that this study will serve as a guide to chemists who wish to access well-defined organonickel complexes with Buchwald-type ligands, the further employment of the ligand class in catalysis, as well as in the design of new ligands and precatalysts for Ni. Additionally, we hope it will enable studies into the many other manifolds of Ni catalysis, including those involving pseudohalide electrophiles, odd oxidation states of Ni, and cationic species, where cation-π interactions between Ni and the B-ring may lead to new reactivity. Additional organometallic studies of the ligand class with Ni, as well as their applications in catalysis, are underway in our lab.

ASSOCIATED CONTENT

Supporting Information

The Supporting Information is available free of charge on the ACS Publications website.

Experimental procedures, experimental data, and characterization and spectral data for new compounds (PDF).

XYZ coordinates for DFT-computed structures (ZIP).

Accession Codes

CCDC 277073–2077078, 2077083, 2077084, 2079498, and 2156651–2156654 contain the supplementary crystallographic data for this paper (CIF). These data can be obtained free of charge via www.ccdc.cam.ac.uk/data_request/cif, or by emailing data–request@ccdc.cam.ac.uk, or by contacting The Cambridge Crystallographic Data Centre, 12 Union Road, Cambridge CB2 1EZ, UK; fax: +44 1223 336033.

AUTHOR INFORMATION

Corresponding Author

Abigail G. Doyle – *Department of Chemistry, Princeton University, Princeton, New Jersey 08544, United States; Department of Chemistry & Biochemistry, University of California Los Angeles, Los Angeles, California 90095, United States*; orcid.org/0000-0002-6641-0833; Email: agdoyle@chem.ucla.edu

Authors

Samuel H. Newman-Stonebraker – *Department of Chemistry, Princeton University, Princeton, New Jersey 08544, United States; Department of Chemistry & Biochemistry, University of California Los Angeles, Los Angeles, California 90095, United States*; orcid.org/0000-0001-6611-8480

Jason Y. Wang – *Department of Chemistry, Princeton University, Princeton, New Jersey 08544, United States; Department of Chemistry & Biochemistry, University of California Los Angeles, Los Angeles, California 90095, United States*; orcid.org/0000-0001-5826-2554

Philip D. Jeffrey – *Department of Molecular Biology, Princeton University, Princeton, New Jersey 08544, United States;* orcid.org/0000-0002-4351-5341

Notes

The authors declare no competing financial interest.

ACKNOWLEDGMENTS

We thank Ken Conover and Dr. Ta-Chung Ong for assistance with low temperature NMR experiments, and Judah Raab, Julia Borowski, Ellyn Peters, and Prof. Matthew Sigman for helpful discussions. Financial support for this work was provided by the NIGMS (R35 GM126986).

REFERENCES

(1) Johansson Seechurn, C. C. C.; Kitching, M. O.; Colacot, T. J.; Snieckus, V. Palladium-Catalyzed Cross-Coupling: A Historical Contextual Perspective to the 2010 Nobel Prize. *Angew. Chem. Int. Ed.* **2012**, *51*, 5062–5085.

(2) Brown, D. G.; Boström, J. Analysis of Past and Present Synthetic Methodologies on Medicinal Chemistry: Where Have All the New Reactions Gone? *J. Med. Chem.* **2016**, *59*, 4443–4458.

(3) Hazari, N.; Melvin, P. R.; Beromi, M. M. Well-Defined Nickel and Palladium Precatalysts for Cross-Coupling. *Nat. Rev. Chem.* **2017**, *1*, 0025

(4) Ruiz-Castillo, P.; Buchwald, S. L. Applications of Palladium-Catalyzed C–N Cross-Coupling Reactions. *Chem. Rev.* **2016**, *116*, 12564–12649.

(5) Surry, D. S.; Buchwald, S. L. Dialkylbiaryl Phosphines in Pd-Catalyzed Amination : A User's Guide. *Chem. Sci.* **2010**, *2*, 27–50.

(6) Martin, R.; Buchwald, S. L. Palladium-Catalyzed Suzuki−Miyaura Cross-Coupling Reactions Employing Dialkylbiaryl Phosphine Ligands. *Acc. Chem. Res.* **2008**, *41*, 1461–1473.

(7) Zapf, A.; Jackstell, R.; Rataboul, F.; Riermeier, T.; Monsees, A.; Fuhrmann, C.; Shaikh, N.; Dingerdissen, U.; Beller, M. Practical Synthesis of New and Highly Efficient Ligands for the Suzuki Reaction of Aryl Chlorides. *Chem. Commun.* **2004**, 38–39.

(8) Rataboul, F.; Zapf, A.; Jackstell, R.; Harkal, S.; Riermeier, T.; Monsees, A.; Dingerdissen, U.; Beller, M. New Ligands for a General Palladium-Catalyzed Amination of Aryl and Heteroaryl Chlorides. *Chem. Eur. J.* **2004**, *10*, 2983–2990.

(9) Strieter, E. R.; Blackmond, D. G.; Buchwald, S. L. Insights into the Origin of High Activity and Stability of Catalysts Derived from Bulky, Electron-Rich Monophosphinobiaryl Ligands in the Pd-Catalyzed C−N Bond Formation. *J. Am. Chem. Soc.* **2003**, *125*, 13978–13980.

(10) Strieter, E. R.; Buchwald, S. L. Evidence for the Formation and Structure of Palladacycles during Pd-Catalyzed C–N Bond Formation with Catalysts Derived from Bulky Monophosphinobiaryl Ligands. *Angew. Chem. Int. Ed.* **2006**, *45*, 925–928.

(11) Barder, T. E.; Walker, S. D.; Martinelli, J. R.; Buchwald, S. L. Catalysts for Suzuki−Miyaura Coupling Processes: Scope and Studies of the Effect of Ligand Structure. *J. Am. Chem. Soc.* **2005**, *127*, 4685–4696.

(12) Barder, T. E.; Biscoe, M. R.; Buchwald, S. L. Structural Insights into Active Catalyst Structures and Oxidative Addition to (Biaryl)Phosphine−Palladium Complexes via Density Functional Theory and Experimental Studies. *Organometallics* **2007**, *26*, 2183–2192.

(13) Ikawa, T.; Barder, T. E.; Biscoe, M. R.; Buchwald, S. L. Pd-Catalyzed Amidations of Aryl Chlorides Using Monodentate Biaryl Phosphine Ligands: A Kinetic, Computational, and Synthetic Investigation. *J. Am. Chem. Soc.* **2007**, *129*, 13001–13007.

(14) Yin, J.; Rainka, M. P.; Zhang, X.-X.; Buchwald, S. L. A Highly Active Suzuki Catalyst for the Synthesis of Sterically Hindered Biaryls: Novel Ligand Coordination. *J. Am. Chem. Soc.* **2002**, *124*, 1162–1163.

(15) Reid, S. M.; Boyle, R. C.; Mague, J. T.; Fink, M. J. A Dicoordinate Palladium(0) Complex with an Unusual Intramolecular η^1-Arene Coordination. *J. Am. Chem. Soc.* **2003**, *125*, 7816–7817.

(16) Biscoe, M. R.; Fors, B. P.; Buchwald, S. L. A New Class of Easily Activated Palladium Precatalysts for Facile C−N Cross-Coupling Reactions and the Low Temperature Oxidative Addition of Aryl Chlorides. *J. Am. Chem. Soc.* **2008**, *130*, 6686–6687.

(17) Yada, A.; Yukawa, T.; Nakao, Y.; Hiyama, T. Nickel/$AlMe_2Cl$-Catalysed Carbocyanation of Alkynes Using Arylacetonitriles. *Chem. Commun.* **2009**, 3931–3933.

(18) Nielsen, D. K.; Doyle, A. G. Nickel-Catalyzed Cross-Coupling of Styrenyl Epoxides with Boronic Acids. *Angew. Chem. Int. Ed.* **2011**, *50*, 6056–6059.

(19) Zhou, Q.; Cobb, K. M.; Tan, T.; Watson, M. P. Stereospecific Cross Couplings To Set Benzylic, All-Carbon Quaternary Stereocenters in High Enantiopurity. *J. Am. Chem. Soc.* **2016**, *138*, 12057–12060.

(20) Ariki, Z. T.; Maekawa, Y.; Nambo, M.; Crudden, C. M. Preparation of Quaternary Centers via Nickel-Catalyzed Suzuki–Miyaura Cross-Coupling of Tertiary Sulfones. *J. Am. Chem. Soc.* **2017**, *140*, 78–81.

(21) Coombs, J. R.; Green, R. A.; Roberts, F.; Simmons, E. M.; Stevens, J. M.; Wisniewski, S. R. Advances in Base-Metal Catalysis: Development of a Screening Platform for Nickel-Catalyzed Borylations of Aryl (Pseudo)Halides with $B_2(OH)_4$. *Organometallics* **2018**, *38*, 157–166.

(22) Munteanu, C.; Spiller, T. E.; Qiu, J.; DelMonte, A. J.; Wisniewski, S. R.; Simmons, E. M.; Frantz, D. E. Pd- and Ni-Based Systems for the Catalytic Borylation of Aryl (Pseudo)Halides with $B_2(OH)_4$. *J. Org. Chem.* **2020**.

(23) Koeritz, M. T.; Burgett, R. W.; Kadam, A. A.; Stanley, L. M. Ni-Catalyzed Intermolecular Carboacylation of Internal Alkynes via Amide C–N Bond Activation. *Org. Lett.* **2020**, *22*, 5731–5736.

(24) Sabater, S.; Menche, M.; Ghosh, T.; Krieg, S.; Rück, K. S. L.; Paciello, R.; Schäfer, A.; Comba, P.; Hashmi, A. S. K.; Schaub, T. Mechanistic Investigation of the Nickel-Catalyzed Carbonylation of Alcohols. *Organometallics* **2020**, *39*, 870–880.

(25) Newman-Stonebraker, S. H.; Smith, S. R.; Borowski, J. E.; Peters, E.; Gensch, T.; Johnson, H. C.; Sigman, M. S.; Doyle, A. G. Univariate Classification of Phosphine Ligation State and Reactivity in Cross-Coupling Catalysis. *Science* **2021**, *374*, 301–308.

(26) Ponce-de-León, J.; Gioria, E.; Martínez-Ilarduya, J. M.; Espinet, P. Ranking Ligands by Their Ability to Ease $(C_6F_5)_2Ni^{II}L \rightarrow Ni^0L + (C_6F_5)_2$ Coupling versus Hydrolysis: Outstanding Activity of PEWO Ligands. *Inorg. Chem.* **2020**, *59*, 18287–18294.

(27) Jacobs, E.; Keaveney, S. T. Experimental and Computational Studies Towards Chemoselective C−F over C−Cl Functionalisation: Reversible Oxidative Addition Is the Key. *ChemCatChem* **2021**, *13*, 637–645.

(28) Marín, M.; Moreno, J. J.; Navarro-Gilabert, C.; Álvarez, E.; Maya, C.; Peloso, R.; Nicasio, M. C.; Carmona, E. Synthesis, Structure and Nickel Carbonyl Complexes of Dialkylterphenyl Phosphines. *Chem. Eur. J.* **2019**, *25*, 260–272.

(29) Martín, M. T.; Marín, M.; Rama, R. J.; Álvarez, E.; Maya, C.; Molina, F.; Nicasio, M. C. Zero-Valent ML_2 Complexes of Group 10 Metals Supported by Terphenyl Phosphanes. *Chem. Commun.* **2021**, *57*, 3083–3086.
(30) Martín, M. T.; Marín, M.; Maya, C.; Prieto, A.; Nicasio, M. C. Ni(II) Precatalysts Enable Thioetherification of (Hetero)Aryl Halides and Tosylates and Tandem C−S/C−N Couplings. *Chem. Eur. J.* **2021**, *27*, 12320–12326
(31) Poater, A.; Cosenza, B.; Correa, A.; Giudice, S.; Ragone, F.; Scarano, V.; Cavallo, L. Samb*V*ca: A Web Application for the Calculation of the Buried Volume of N-Heterocyclic Carbene Ligands. *Eur. J. Inorg. Chem.* **2009**, 1759–1766.
(32) Clavier, H.; Nolan, S. P. Percent Buried Volume for Phosphine and N-Heterocyclic Carbene Ligands: Steric Properties in Organometallic Chemistry. *Chem. Commun.* **2010**, *46*, 841–861.
(33) Falivene, L.; Cao, Z.; Petta, A.; Serra, L.; Poater, A.; Oliva, R.; Scarano, V.; Cavallo, L. Towards the Online Computer-Aided Design of Catalytic Pockets. *Nat. Chem.* **2019**, *11*, 872–879.
(34) Gensch, T.; Gomes, G. dos P.; Friederich, P.; Peters, E.; Gaudin, T.; Pollice, R.; Jorner, K.; Nigam, A.; Lindner-D'Addario, M.; Sigman, M. S.; Aspuru-Guzik, A. A Comprehensive Discovery Platform for Organophosphorus Ligands for Catalysis. *J. Am. Chem. Soc.* **2022**, *144*, 1205–1217.
(35) Standley, E. A.; Smith, S. J.; Müller, P.; Jamison, T. F. A Broadly Applicable Strategy for Entry into Homogeneous Nickel(0) Catalysts from Air-Stable Nickel(II) Complexes. *Organometallics* **2014**, *33*, 2012–2018.
(36) Niemeyer, Z. L.; Milo, A.; Hickey, D. P.; Sigman, M. S. Parameterization of Phosphine Ligands Reveals Mechanistic Pathways and Predicts Reaction Outcomes. *Nat. Chem.* **2016**, *8*, 610–617.
(37) Bajo, S.; Laidlaw, G.; Kennedy, A. R.; Sproules, S.; Nelson, D. J. Oxidative Addition of Aryl Electrophiles to a Prototypical Nickel(0) Complex: Mechanism and Structure/Reactivity Relationships. *Organometallics* **2017**, *36*, 1662–1672.
(38) Greaves, M. E.; Humphrey, E. L. B. J.; Nelson, D. J. Reactions of Nickel(0) with Organochlorides, Organobromides, and Organoiodides: Mechanisms and Structure/Reactivity Relationships. *Catal. Sci. Technol.* **2021**, *11*, 2980–2996.
(39) PhJohnPhos was also subjected to these spectroscopic studies, and it was observed that it reacted with $Ni(COD)_2$ to form $Ni(PhJohnPhos)_2$. Single crystals of this complex were obtained directly from the reaction mixture, confirming its identity (see SI for more information).
(40) Even for the ligands that were able to spectroscopically form ligated complexes, the conversions were generally low (<20%).
(41) Velian, A.; Lin, S.; Miller, A. J. M.; Day, M. W.; Agapie, T. Synthesis and C−C Coupling Reactivity of a Dinuclear Ni^{I}–Ni^{I} Complex Supported by a Terphenyl Diphosphine. *J. Am. Chem. Soc.* **2010**, *132*, 6296–6297.
(42) Herbert, D. E.; Lara, N. C.; Agapie, T. Arene C–H Amination at Nickel in Terphenyl-Diphosphine Complexes with Labile Metal-Arene Interactions. *Chem. Eur. J.* **2013**, *19*, 16453–16460.
(43) Nattmann, L.; Saeb, R.; Nöthling, N.; Cornella, J. An Air-Stable Binary Ni(0)–Olefin Catalyst. *Nat. Catal.* **2019**, 1–8.
(44) Lutz, S.; Nattmann, L.; Nöthling, N.; Cornella, J. 16-Electron Nickel(0)-Olefin Complexes in Low-Temperature C(Sp2)–C(Sp3) Kumada Cross-Couplings. *Organometallics* **2021**, *40*, 2220–2230.
(45) Tran, V. T.; Li, Z.; Apolinar, O.; Derosa, J.; Joannou, M. V.; Wisniewski, S. R.; Eastgate, M. D.; Engle, K. M. Ni(COD)(DQ): An Air-Stable 18-Electron Nickel(0)–Olefin Precatalyst. *Angew. Chem. Int. Ed.* **2020**, *59*, 7409–7413.
(46) Similar results observed with 4-chlorobenzotrifluoride and 4-chloroanisole, though decomposition to Ni black was significantly greater, and additional paramagnetic species were observed.
(47) Zhu, S.; Shoshani, M. M.; Johnson, S. A. Versatile (η^6Arene)Ni(PCy_3) Nickel Monophosphine Precursors. *Chem. Commun.* **2017**, *53*, 13176–13179.
(48) NMR analysis of recrystallized **1** in the absence of additional free ligand shows partial ligand dissociation in a 1:1 ratio with a new resonance by ^{31}P NMR, suspected to be the $L_1Ni(0)$ dimer of **i**. Addition of 2 equiv of free ligand to this solution does not decrease the intensity of the peak attributed the dissociation product, which appears to form irreversibly. However, addition of 2 equiv of free ligand to solid **1** *prior* to its dissolution results in no observed dissociation product, giving further experimental support of the intermediacy of **i**.
(49) Jongbloed, L. S.; García-López, D.; van Heck, R.; Siegler, M. A.; Carbó, J. J.; van der Vlugt, J. I. Arene $C(Sp^2)$-H Metalation at Ni^{II} Modeled with a Reactive $PONC_{Ph}$ Ligand. *Inorg. Chem.* **2016**, *55*, 8041–8047.
(50) Omer, H. M.; Liu, P. Computational Study of the Ni-Catalyzed C–H Oxidative Cycloaddition of Aromatic Amides with Alkynes. *ACS Omega* **2019**, *4*, 5209–5220.
(51) Mangin, L. P.; Zargarian, D. C–H Nickelation of Aryl Phosphinites: Mechanistic Aspects. *Organometallics* **2019**, *38*, 1479–1492.
(52) Mangin, L. P.; Zargarian, D. C–H Nickelation of Naphthyl Phosphinites: Electronic and Steric Limitations, Regioselectivity, and Tandem C–P Functionalization. *Organometallics* **2019**, *38*, 4687–4700.
(53) Mangin, L. P.; Zargarian, D. C–H Nickellation of Phenol-Derived Phosphinites: Regioselectivity and Structures of Cyclonickellated Complexes. *Dalton Trans.* **2017**, *46*, 16159–16170.
(54) Vabre, B.; Lambert, M. L.; Petit, A.; Ess, D. H.; Zargarian, D. Nickelation of PCP- and POCOP-Type Pincer Ligands: Kinetics and Mechanism. *Organometallics* **2012**, *31*, 6041–6053.
(55) Vabre, B.; Deschamps, F.; Zargarian, D. Ortho Derivatization of Phenols through C–H Nickelation: Synthesis, Characterization, and Reactivities of Ortho-Nickelated Phosphinite Complexes. *Organometallics* **2014**, *33*, 6623–6632.
(56) Volpe, E. C.; Chadeayne, A. R.; Wolczanski, P. T.; Lobkovsky, E. B. Heterolytic CH-Bond Activation in the Synthesis of $Ni\{(2\text{-Aryl-}\kappa C^2)\text{Pyridine-}\kappa N\}_2$ and Derivatives. *J. Organomet. Chem.* **2007**, *692*, 4774–4783.
(57) Chong, E.; Kampf, J. W.; Ariafard, A.; Canty, A. J.; Sanford, M. S. Oxidatively Induced C–H Activation at High Valent Nickel. *J. Am. Chem. Soc.* **2017**, *139*, 6058–6061.
(58) Given that approximately half of the Ni decomposes, it is feasible that the mechanism proceeds via a sacrificial bimolecular pathway and/or involves Ni(I) species.
(59) Payard, P.-A.; Perego, L. A.; Ciofini, I.; Grimaud, L. Taming Nickel-Catalyzed Suzuki-Miyaura Coupling: A Mechanistic Focus on Boron-to-Nickel Transmetalation. *ACS Catal.* **2018**, *8*, 4812–4823.
(60) Thomas, A. A.; Denmark, S. E. Pre-Transmetalation Intermediates in the Suzuki-Miyaura Reaction Revealed: The Missing Link. *Science* **2016**, *352*, 329–332.
(61) Thomas, A. A.; Wang, H.; Zahrt, A. F.; Denmark, S. E. Structural, Kinetic, and Computational Characterization of the Elusive Arylpalladium(II)Boronate Complexes in the Suzuki–Miyaura Reaction. *J. Am. Chem. Soc.* **2017**, *139* (10), 3805–3821.
(62) Christian, A. H.; Müller, P.; Monfette, S. Nickel Hydroxo Complexes as Intermediates in Nickel-Catalyzed Suzuki–Miyaura Cross-Coupling. *Organometallics* **2014**, *33*, 2134–2137.
(63) In computational studies, Espinet and coworkers found that THF could stabilize Ni(II) species with CyJohnPhos (see reference 26). Under the catalytic conditions, it is likely that solvent and/or water may bind as an L-type ligand, which would also require the phosphine to adopt a low %Vbur conformation with the B-ring rotated out of the coordination site.
(64) The most stable conformations for CyJohnPhos during the transmetalation steps had %Vbur values a few percent above $\%V_{bur}$ (*min*) of 32%. In these structures, the unsubstituted B-ring was positioned >3 Å above (or below) the Ni xy-plane (i.e., monodentate) with stabilizing C–H ⋯ π interactions observed between the hydrogens of the Ni-bound aryl group and the π-face of the B-ring. See SI for details.
(65) Biscoe, M. R.; Barder, T. E.; Buchwald, S. L. Electronic Effects on the Selectivity of Pd-Catalyzed C–N Bond-Forming Reactions Using Biarylphosphine Ligands: The Competitive Roles of Amine Binding and Acidity. *Angew. Chem. Int. Ed.* **2007**, *46*, 7232–7235.
(66) Düfert, M. A.; Billingsley, K. L.; Buchwald, S. L. Suzuki-Miyaura Cross-Coupling of Unprotected, Nitrogen-Rich Heterocycles: Substrate Scope and Mechanistic Investigation. *J. Am. Chem. Soc.* **2013**, *135*, 12877–12885.
(67) Wolfe, J. P.; Buchwald, S. L. Nickel-Catalyzed Amination of Aryl Chlorides. *J. Am. Chem. Soc.* **1997**, *119*, 6054–6058.

(68) Lavoie, C. M.; Stradiotto, M. Bisphosphines: A Prominent Ancillary Ligand Class for Application in Nickel-Catalyzed C–N Cross-Coupling. *ACS Catal.* **2018**, *8*, 7228–7250.
(69) Liu, R. Y.; Dennis, J. M.; Buchwald, S. L. The Quest for the Ideal Base: Rational Design of a Nickel Precatalyst Enables Mild, Homogeneous C–N Cross-Coupling. *J. Am. Chem. Soc.* **2020**, *142*, 4500–4507.
(70) Lavoie, C. M.; MacQueen, P. M.; Rotta-Loria, N. L.; Sawatzky, R. S.; Borzenko, A.; Chisholm, A. J.; Hargreaves, B. K. V.; McDonald, R.; Ferguson, M. J.; Stradiotto, M. Challenging Nickel-Catalysed Amine Arylations Enabled by Tailored Ancillary Ligand Design. *Nat. Commun.* **2016**, *7*, 11073.
(71) Clark, J. S. K.; Ferguson, M. J.; McDonald, R.; Stradiotto, M. PAd2-DalPhos Enables the Nickel-Catalyzed C−N Cross-Coupling of Primary Heteroarylamines and (Hetero)Aryl Chlorides. *Angew. Chem. Int. Ed.* **2019**, *58*, 6391–6395.
(72) Lavoie, C. M.; Tassone, J. P.; Ferguson, M. J.; Zhou, Y.; Johnson, E. R.; Stradiotto, M. Probing the Influence of PAd-DalPhos Ancillary Ligand Structure on Nickel-Catalyzed Ammonia Cross-Coupling. *Organometallics* **2018**, *37*, 4015–4023.
(73) Clevenger, A. L.; Stolley, R. M.; Aderibigbe, J.; Louie, J. Trends in the Usage of Bidentate Phosphines as Ligands in Nickel Catalysis. *Chem. Rev.* **2020**, *120*, 6124–6196.
(74) Zhang, S.; Li, X.; Sun, H. Selective Amination of Aryl Chlorides Catalysed by $Ni(PMe_3)_4$. *Dalton Trans.* **2015**, *44*, 16224–16227.
(75) Hu, H.; Burlas, C. E.; Curley, S. J.; Gruchala, T.; Qu, F.; Shaughnessy, K. H. Effect of Aryl Ligand Identity on Catalytic Performance of Trineopentylphosphine Arylpalladium Complexes in N-Arylation Reactions. *Organometallics* **2020**, *39*, 3618–3627.
(76) Malapit, C. A.; Borrell, M.; Milbauer, M. W.; Brigham, C. E.; Sanford, M. S. Nickel-Catalyzed Decarbonylative Amination of Carboxylic Acid Esters. *J. Am. Chem. Soc.* **2020**, *142*, 5918–5923.
(77) Simon, C. M.; Dudra, S. L.; McGuire, R. T.; Ferguson, M. J.; Johnson, E. R.; Stradiotto, M. Identification of a Nitrenoid Reductive Elimination Pathway in Nickel-Catalyzed C–N Cross-Coupling. *ACS Catal.* **2022**, *12*, 1475–1480.
(78) Till, N. A.; Tian, L.; Dong, Z.; Scholes, G. D.; MacMillan, D. W. C. Mechanistic Analysis of Metallaphotoredox C–N Coupling: Photocatalysis Initiates and Perpetuates Ni(I)/Ni(III) Coupling Activity. *J. Am. Chem. Soc.* **2020**, *142*, 15830–15841.
(79) For BrettPhos, it is known with Pd that the ligand can adopt conformations wherein the 3-OMe of the A-ring is bound to the metal, adopting it's minimum %Vbur (min) conformer of 35%. While we have not ruled out its possibility in Reaction IV, or in Ni catalysis more generally, this binding mode would also effectively make the ligand bidentate, as the OMe group fully occupies a second coordination site on the metal.

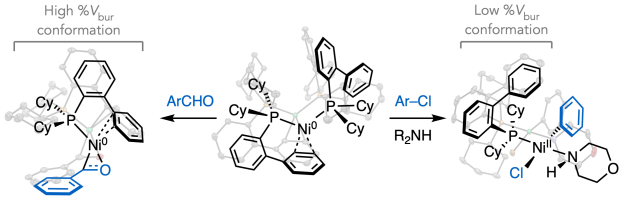

- *Access to well-defined Ni(0) and Ni(II) complexes with Buchwald-type ligands*
- *Structure-reactivity relationship studies for four cross-coupling datasets*